Proceedings of PVP'01:
2001 ASME Pressure Vessels and Piping Conferences
July 22 – 26, 2001, Atlanta, Georgia, USA

PVPTC01/DAC-1234

A NUMERICAL STUDY OF STRATIFIED LAYERS IN VENTILATED ENCLOSURES

Konstantinos Pikos*
Fluid Mechanics Research Group, ACME Dept.,
University of Hertfordshire, Hatfield, AL10 9AB, UK.
k.pikos@herts.ac.uk

Rajnish K. Calay
Fluid Mechanics Research Group, ACME Dept.,
University of Hertfordshire, Hatfield, AL10 9AB, UK.
r.k.calay@herts.ac.uk

ABSTRACT

The present study is a numerical investigation of buoyancy-dominated flow leading to stratification in ventilated spaces. Air is supplied through inlets at floor and ceiling at different temperatures and an exhaust duct is located on the right wall. Different arrangements of the exhaust height are studied to evaluate its effect on velocity and temperature distribution and stratification in the room. Three-dimensional model is used to predict distribution of air velocity, temperature and turbulent kinetic energy. In stratified shear flows the modeling of vertical disturbances is most important in the evolution of turbulence. Thus to model the production, dissipation and transport of turbulence, three different models were used, the standard k–ε model, the kchen model and the RNG k–ε model to evaluate the standard approaches used in room ventilation modeling by predicting the mean flow field. Richardson number (Ri) criterion is used to investigate the preservation and break up of temperature-stratified interface in a stratified enclosed environment.

NOMENCLATURE

A cross-sectional area
Ar Archimedes number
B width of room
C_μ, C_1, C_2, C_3, $C_{1\varepsilon}$, $C_{2\varepsilon}$ turbulent constants
G_B buoyancy destruction term
D_h hydraulic diameter
f_1 Lam-Bremhorst (1981) dumping function
Gr Grashof number $\left(=\frac{gl^3\beta\Delta t}{\nu^2}\right)$
G_f Total exchange coefficient
H height of room
k turbulent kinetic energy
L characteristic length
P pressure
P_K shear production rate
Pr Prandtl number
Re Reynolds number $\left(\frac{\rho u l}{\mu}\right)$
Ri Overall Richardson number
Ri_g Gradient Richardson number
S_{ij} Stress tensor
S_ε Source term
T temperature
t normalized temperature
T_H Temperature of Hot Air Supply
T_C Temperature of Cold Air Supply
U Characteristic velocity
u,v mean velocity components
u_τ friction velocity
V volumetric flow rate
W length of room
x,y cartesian coordinates
y^+ dimensionless distance from wall (= uy/ν)

Greek symbols
ε turbulent dissipation rate
λ thermal conductivity
μ molecular viscosity
μ_e effective viscosity
μ_t eddy viscosity
ν_t turbulent dynamic viscosity
σ_t turbulent Prandtl number
σ_k,σ_ε turbulent Schmidt numbers

* Address all correspondence to this author. Tel.: +44-1707-284942; fax: +44-1707-285086.

Subscripts

$_0$	inlet, characteristic
$_e$	effective
$_S$	supply
$_x$	at exhaust duct
$_H$	hot air supply
$_C$	cold air supply

INTRODUCTION

Stratification due to temperature gradient is important phenomenon in single cell buildings because it significantly influences the efficiency of ventilation and air-conditioning systems. In the design of energy-efficient ventilation systems, generally efforts are made to de-stratify the flow in order to achieve uniform desired air temperature and to reduce the heating load of the building. But there are situations where stratification is positively used in the design of ventilation or air-conditioning systems. For example, stratification effects are utilized to reduce the cooling load of the building air-conditioning system (Allen, 1979). There are types of ventilation systems such as displacement ventilation (Nielsen *et al.*, 1994; Mundt, 1995) and selective ventilation which utilize the properties of stratified flow (Skistad, 1998; Calay *et al.*, 2000). In fire scenarios the spread of smoke is also influenced by thermal stratification. Therefore, for better ventilation design and smoke management the understanding of stratified flow in buildings is important.

Although a vast number of studies are available on stratification, such as geophysical, oceanic and atmospheric stratification dealing with the effects of seismic waves, water waves and atmospheric waves on the stratification of the fluid (Linden, 1980; Redondo *et al.*, 1996), very little information on stratification is available in relation to buildings. Many numerical studies of flow in buildings have been reported in the literature (Murakami *et al.*, 1989, Ohira *et al.*, 2000). However, there are issues yet to be resolved relating to choosing appropriate boundary conditions, mesh resolutions and turbulence models for flows dominated by buoyancy and stratification.

The present study considers the simulation of air movement in ventilated spaces. The influence of heat sources is not present to create stratification in the room. Therefore, in order to create stratification or stratified flow, a temperature differential was created across the room height by supplying warm air from the ceiling.

BACKGROUND

Modeling Flow Phenomena In Stratified Flows

In order to understand stratification in enclosed spaces it is necessary to outline and understand all the phenomena occurring in such enclosures paying particular attention to the sources that build stratification. In our case such sources are the air supplies in the room which can produce jet-like flows which can mix the enclosed medium and destabilize it. Even at very low Reynolds numbers there will be some mixing in the surrounding medium of the supply jet. The entrainment of the jet is proportional to its centreline velocity and the area of the emerging supply. The jet flow is divided into zones, core transition and termination zone from which the last one determines where the jet damps its properties. In the case of a buoyant jet, the body forces are the basic mechanism for driving the flow such that the fluid motion can be categorised as 'plume' of laminar velocity. However, in isothermal jet flows there is a transitional velocity at which the jet will become a plume. Providing that jet-like velocities do not exceed a certain Reynolds number the medium will not suffer from the mixing effects of the jet. In contrast to the warm air supply, the effects utilized by the cold air supply will be more jet like. Due to its high density, cold air will be discharged to the floor level, leaving unaffected most of the higher up warmer air. Thus it would be sensible if the supply of cool air were allocated at the floor level aiming to cooling the occupied zone.

Stability Criteria

There are a number of different stability criteria used in the past to characterize the stability of stratified flows in lakes, estuaries and the atmosphere. For flows at very low Reynolds number, where the viscous damping will reduce the growth rate of disturbances, stability can be expressed by the Keulegan number. The Kelvin-Helmholz stability is a more general case where fluids of different densities lie at different levels and characterizes the stability of overturning of fluid which is described by the Richardson number, which is adopted here in describing the stability of stratification.

The Richardson number is a measure of the buoyancy force to inertia force due to turbulence acting on the fluid. Thus, local gradient Richardson number can be expressed as,

$$Ri_g = \frac{-g\left(\frac{\delta\rho}{\delta z}\right)}{\rho\left(\frac{\delta u}{\delta z}\right)^2} \qquad (1)$$

where the minus sign is due to density decreases with height. Negative Ri_g corresponds to destabilizing density gradient where both shear and buoyancy give rise to turbulence, i.e., when density increases upwards the buoyancy provides additional source of turbulence. Ri_g is zero for non-stratified flows and increases with strength of stratification.

When density variations are due to temperature variations, Ri_g can be expressed in terms of temperature gradient,

$$Ri_g = \frac{g\beta\left(\frac{\delta t}{\delta z}\right)}{\rho\left(\frac{\delta u}{\delta z}\right)^2} \quad (2)$$

where β is the volumetric expansion coefficient denoted by the reciprocal of the reference temperature.

Perturbation analysis has shown that a laminar layer of stratified fluid is stable with respect to small perturbations if the local Richardson number, Ri_g, exceeds ¼ everywhere in the flow. If Ri_g becomes lower than ¼ at any part, the shear across the interface becomes so large that the stable density gradient no longer will be able to stabilize the flow. This does not however necessarily imply that in an existing turbulent shear flow, the turbulence would disappear if Ri_g exceeds ¼. In fact it seems to be possible for turbulence to exist even when the overall Richardson number is well above ¼. Based on the overall Richardson number a turbulent shear layer is expected to laminarise if,

$$\frac{1}{4} < Ri = \frac{\Delta\rho}{\rho}\frac{L}{(\Delta u)^2} \le 1 \quad (3)$$

where L is the characteristic length scale of the room.

In general, stability is likely to occur if $Ri > 1$.

Similarity Criteria

Archimedes number, Ar, is conventionally used as a non-dimensional number to characterize non-isothermal flows in buildings. Parametric studies are performed for a range of Ar to investigate its effect on velocity and temperature distribution. Ar number is the ratio of buoyancy force to the inertial force. Thus in terms of density variation one has,

$$Ar = \frac{gl\Delta\rho}{\rho u^2}. \quad (4)$$

In the case of natural motion of air Ar can be transformed so that it no longer contains the velocity term in the explicit form. When Archimedes number is related to stability criteria, then it can be expressed as the ratio of the buoyancy force to the viscous force,

$$Gr = \frac{gl^3\Delta\rho\,\rho^2}{\rho\,\mu^2}. \quad (5)$$

the above relation is obtained multiplying Ar by Reynolds number. Reynolds number gives the relation of inertia force to viscous force, which is defined as,

$$Re = \frac{\rho u l}{\mu} \quad (6)$$

thus, combining equations (4), (5) and (6) yields to the following relation,

$$Ar = \frac{Gr}{Re^2} \quad (7)$$

where l is the hydraulic diameter of the room, D_h, denoted as,

$$D_h = \frac{2BH}{B+H} \quad (8)$$

Temperature is normalized by the ratio of the output heat load in the middle of the room over the input heat load,

$$t = \frac{(T - T_C)}{(T_H - T_C)}. \quad (9)$$

GEOMETRY OF THE MODEL

The geometry of a simulated room environment is depicted in Schematic 1.

NUMERICAL MODEL

The eddy viscosity concept is employed in the current numerical experiments. In the past two decades the k–ε model and its modifications have been very popular for simulating the turbulence effects of very large flow domains and complex geometries and has been used for a wide range of industrial application which was in a good agreement compare to experimental data. Three versions of k–ε model were used. Besides the standard high-Reynolds number one, kchen model and the Renormalization Group (RNG) model were also used. The simulations are performed steady-state by using CFD (Computational Fluid Dynamics) package PHOENICS version 3.3 which employs the Navier-Stokes equations,

$$\rho u_j \frac{\partial u_i}{\partial x_j} = -\frac{\partial P}{\partial x_i} + \frac{\partial}{\partial x_j}\left[\mu_e\left(\frac{\partial u_i}{\partial x_j} + \frac{\partial u_j}{\partial x_i}\right)\right] - \rho g\beta(T - T_0) \quad (10)$$

the energy equation,

$$\rho u_j \frac{\partial T}{\partial x_j} = \frac{\partial}{\partial x_j}\left[G_f\left(\frac{\partial T}{\partial x_j}\right)\right] \quad (11)$$

and the continuity equation,

$$\rho \frac{\partial u_j}{\partial x_j} = 0 . \quad (12)$$

In the equations above, μ_e is the effective viscosity,

$$\mu_e = \mu + \mu_t \quad (13)$$

and G_f is the total exchange coefficient and it is the sum of the laminar and turbulent exchange coefficients,

$$G_f = \frac{\mu}{Pr} + \frac{\mu_t}{\sigma_t} . \quad (14)$$

The Standard *k–ε* Model

Initially, the standard high-Reynolds-number *k–ε* model is used paper as presented by Launder and Spalding (1974) with inclusion of allowance for buoyancy effects to simulate room air motion. Turbulent viscosity is defined as follows,

$$\mu_t = \rho C_\mu \frac{k^2}{\varepsilon} \quad (15)$$

where C_μ is an empirical constant.

There are two extra equations for turbulent kinetic energy and dissipation,

$$\rho \frac{\partial k}{\partial t} + \left(\rho u_i k - \rho \frac{\nu_t}{\sigma_k} k_{,i} \right)_{,i} = \rho \left(P_K + G_B - \varepsilon \right) \quad (16)$$

$$\rho \frac{\partial \varepsilon}{\partial t} + \left(\rho u_i \varepsilon - \rho \frac{\nu_t}{\sigma_\varepsilon} \varepsilon_{,i} \right)_{,i} = \left(\rho \frac{\varepsilon}{k} \right) \left(C_1 P_K + C_3 G_B - C_2 \varepsilon \right) \quad (17)$$

where P_K is the shear production, i.e., the volumetric production rate of turbulent kinetic energy by shear forces. This is defined as follows,

$$P_K = \nu_t \left(u_{i,j} + u_{j,i} \right) u_{i,j} \quad (18)$$

and G_B is the destruction by buoyancy term , i.e. the volumetric production rate of turbulent kinetic energy by gravitational forces interacting with density gradients,

$$G_B = -g_i \frac{\nu_t}{\sigma_t} \frac{\rho_{,i}}{\rho} \quad (19)$$

where g_i is the gravitational vector and σ_t is the turbulent Prandtl number.

G_B is negative for stably-stratified flows, so that dense layers of fluid can flow below light layers without mixing, and thus kinetic energy is reduced and turbulence is damped. Whereas G_B is positive for unstably-stratified flows where dense layers of fluid exist above light layers, so that kinetic energy is increased at the expense of potential energy of the gravitational force. The Boussinesq approximation is employed, in which the variations in density are expressed by way of variations in temperature. For a stably-stratified condition equation (14) reduces to:

$$G_B = \beta g_{,i} \frac{\nu_t}{\sigma_t} T_{,i} \quad (20)$$

The following constants are universally used for the standard *k–ε* model, $\sigma_k = 1.0$, $\sigma_\varepsilon = 1.314$, $C_\mu = 0.09$, $C_1 = 1.44$, $C_2 = 1.92$, $C_3 = 1.0$.

The kchen Model

The kchen model is derived by Chen and Kim (1987) which is a modified version of the *k–ε* model. The kchen modification involves dividing the dissipation production term into two parts, the first of which is the same as for the standard model but with a smaller multiplying coefficient, C_1. The second part allows the "turbulence distortion ratio" (P_K/ε) to exert an influence on the production rate of ε.

The net effect is to increase ε (and thereby decrease k) when the mean strain is strong ($P_K/\varepsilon > 1$), and to decrease ε when the mean strain is weak ($P_K/\varepsilon < 1$). This feature may be expected to offer advantages in separated flows and also in other flows where the turbulence is removed from local equilibrium. To account for such effects, an extra timescale k/P_K is included in the ε equation via the following additional source term per unit volume,

$$S_\varepsilon = \rho f_1 C_{3\varepsilon} P_k^{2/k} \quad (21)$$

where f_1 is the Lam-Bremhorst (1981) dumping function.

The authors claim that the extra source term represents the energy transfer rate from large-scale to small-scale turbulence controlled by the production-range time scale and the dissipation-range timescale. Meaning that kchen model gives similar results compare to the standard model for simple flows and makes better predictions for complex flows involving recirculation and streamline curvature and swirl.

Chen extended the model to perform for low-Reynolds-number simulations of bounded flows by introducing the low-Reynolds-number *k–ε* extension. The following model constants are used instead of the standard ones in the *k–ε* model, $\sigma_k = 0.75$, $\sigma_\varepsilon = 1.15$, $C_{1\varepsilon} = 1.15$, $C_{2\varepsilon} = 1.9$, $C_{3\varepsilon} = 0.25$.

Non-Linear RNG *k–ε* Model

This model is derived from the *k–ε* model based on the Renormalization Group (RNG) methods. Similar, to the kchen model, RNG model employs additional sink/source terms in the ε equation and different values for the model constants. The following source term is added in the ε equation,

$$-\frac{C_\mu \eta^3 (1-\eta/\eta_0)}{1+\beta\eta^3}\frac{\varepsilon^2}{k}. \qquad (22)$$

In the above term the parameter η is the ratio of time scales of turbulence to the mean flow fields,

$$\eta = S\frac{k}{\varepsilon} \qquad \text{where} \qquad S = \sqrt{2S_{ij}S_{ij}} = \sqrt{P_K/\mu_t}$$

η_0 is the fixed point for homogeneously-strained turbulent flows and β here is a constant evaluated to yield a von Karman constant of about 0.41.

The different model constants in this model are the following, σ_k = 0.7194, σ_ε = 0.7194, $C_{1\varepsilon}$ = 1.42, $C_{2\varepsilon}$ = 1.68, C_μ = 0.0845.

Near-Wall Modeling

Wall functions that provide the boundary conditions for the mean-flow and the turbulence transport equations for the viscous sublayer are employed for near wall modeling. In such a way, the wall shear stress is connected to the dependent variables in the first point away from the wall where in fully turbulent fluid the outer edge of the near wall element is presumed to lie outside the viscous sublayer. The advantages of this approach are that it escapes the need to extend the computations right down to the wall, and avoids the need to account for viscous effects in the turbulence model

The following wall functions are those appropriate to a inner wall layer in local equilibrium,

$$u^+ = \frac{u_r}{u_\tau} = \frac{1}{\kappa}\ln(Ey^+) \qquad (23)$$

$$k = {u_\tau}^{2/\sqrt{C_\mu}} \qquad (24)$$

$$\varepsilon = C_\mu^{\frac{3}{4}} k^{1.5/\kappa y} \qquad (25)$$

where u+ is the inner variable for velocity and relates u_r, which is the absolute value of the resultant velocity parallel to the wall at the first grid node, and u_τ, the resultant friction velocity,

$$u_\tau = \sqrt{\nu\left(\frac{\partial u}{\partial y}\right)_w} = \sqrt{\nu\frac{|u|}{y}} \qquad (26)$$

y is the normal distance of the first grid point from the wall, y^+ is the dimensionless wall distance $u_\tau y/\nu$ or cell Reynolds number, C_μ (=0.09) is the standard constant in the *k–ε* model, κ (=0.41) is the von Karman constant and E (=8.6) is a wall-roughness parameter.

Equation (24) is the well-known logarithmic law of the wall, and strictly this law should be applied to a point whose y^+ value is in the range $30 < y^+ < 130$.

The boundary condition for *k* assumes that the turbulence is in local equilibrium and consequently, this set of wall functions is not really suitable under separated conditions, as turbulent energy diffusion towards the wall is significant, leading to appreciable departures from local equilibrium.

NUMERICAL EXPERIMENTS

A series of steady-state numerical simulations were performed using the standard *k–ε* model, the kchen extension and the RNG *k–ε* model. The simulations were carried out on a PC-550MHz Pentium III with 1GB RAM physical memory. The geometry of the model is depicted in Schematic 1. Uniform inlet boundary conditions are applied to both hot and cold air supplies. The inlet velocities vary from 0.2 m/s to 1.6 m/s, which is approximately from 3 to 25 air changes per hour (ACH) and the inlet temperatures from 10°C to 40°C modifying the Reynolds number at the inlets respectively as tabulated in Table 1. The initial simulations were performed from 10°C to 30°C. However, *Ar* similarity was observed for the range of these tests with 20°C to 40°C range tests. Initially, different turbulent kinetic levels were set at the inlets and the results from the standard *k–ε* model were compared to the experimental observations made by Calay *et al.* (2000). The computational grid dimensions that described the problem best were 42×63×36. Convergence was achieved very fast, in some cases even 1-2 orders before the 500th iteration. A ratio for convergence was set to 0.1%.

RESULTS AND DISCUSSION

The flow at the supply can be characterized as turbulent whereas the flow in the room away from the supplies is fairly laminar and only low frequency fluctuations can be observed in the velocity field.

The simulation results in Figure 1 and Figure 2 at different *Ar* numbers show a combination of both displacement and mixed ventilation which is achieved by supplying hot air at the ceiling and cold air at floor level. The flow pattern of the cold air supply is that of a wall jet. The velocity decreases linearly with distance cooling the whole of the occupied space up to the

opposite wall where a low velocity circulation is formed. Circulating flow is inherent due to the entrainment of the cold jet. The hot air jet is confined close to the wall where a circulation is formed. The wake of the hot jet terminates at some distance below the top of the interface where hot air is buoyed up and the momentum forces encounter buoyancy forces in the opposite direction. As a result, there is a circulation of hot air in the unconfined side of the hot jet. At that instance, some of the buoyed air is re-circulated back to the hot air jet by the entrainment process, whereas at the same time buoyed air is buoyed under the ceiling towards the exhaust.

An interface of sharp elevated temperatures is formed at the exhaust height where the velocity vectors point towards the exhaust. Looking at Figure 2, the interface height changes in proportion to the exhaust height whereas the thickness of the interface stays approximately the same.

Looking now at Figure 1, it can be seen that the interface thickness changes in proportion to inlet supplies. As it can be seen from the simulation, there is a threshold value where the flow media mixes and stratification is no longer an issue.

Mixing is inherent even at very low inlet supply velocities as low as 0.2 m/s in the current work. However, turbulence is not dominant and thus it does not have a significant effect on stratified flow. This is not valid when overall *Ri* number is below 0.6 or inlet velocities exceed 1.2 – 1.6 m/s in the current work.

Temperature gradient across the room height is well predicted by all eddy viscosity models used in this work as shown in Figure 1 (a), (b), (c) and (d). The standard *k–ε* model is in close agreement with kchen model, for low *Re* numbers and this can be seen in Figure 4 (a), Figure 5 (a) and Figure 6 (a). However in this case, RNG model is more distinctive towards the prediction of the interface. In Figure 4 (a)the RNG model predicts the predominant velocity close to the layer in a similar way to the *k–ε* model, while in Figure 5 (a), it is obvious that RNG model predicts higher vertical disturbances in the opposite direction due to the weakness of the model in calculating the C_μ value in the laminar regimes. The turbulence kinetic level predictions as shown in Figure 6 are higher in the case of the *k–ε* models than any other case.

The kchen model is very close to *k–ε* in all cases. The small deviation in the values is due to the non-uniformities in the flow field. The shear production is overpredicted by the *k–ε* in the low velocity regions which have an effect on local mixing. The kchen model overpredicts the extend of the separation region in the case of the highest *Re* number.

Changing the exhaust height has an effect on the interface height. The hot plume as predicted by the RNG model shows a more defused whereas in the case of *k–ε* the variation in temperature is smoother.

CONCLUSIONS

Although all models are in close agreement with each other, the *k–ε* model gives a more reliable prediction of the mixing in the interface.

The physics of the flow are well predicted. The hot jet from the ceiling is buoyed up when it reaches the height of the interface where buoyancy forces dominate gravitational forces and the momentum of the impinging plum on the stratified interface which is well defined by all models.

From the simulation it is also shown that the interface height is directly proportional to the exhaust height for room temperatures. Additionally, a direct relation is also present between interface thickness and supply velocity.

REFERENCES

Allen, C. J., 1979, "Stratification by design", *ASHRAE J.*, Vol. 21, No. 4, pp. 32-34, April.

Calay, R.K., Børresen, B.A., Holdø, A.E., 2000, "Selective ventilation in large enclosures", Energy and Buildings, Vol. 32, issue 3, pp. 281-289, November.

Chen, Y.S. and Kim, S.W., 1987, "Computation of turbulent flows using an extended *k–ε* turbulence closure model", NASA CR-179204.

Dagestad, S., 1991, "Numerical simulation of stratified flows with different *k–ε* turbulence models", PhD thesis, University of Trondheim.

Launder, B.E. and Spalding, D.B., 1974, "The numerical computation of turbulent flows", *Comp. Meth. in Appl. Mech. & Eng.*, Vol. 3, pp. 269.

Linden, P.F., 1980, "Mixing across a density interface produced by grid turbulence", *Journal of Fluid Mechanics*, Vol. 100, Part 4, pp. 691-703, Oct.

Mundt, E., 1995, "Displacement ventilation systems – Convection flows and Temperature Gradients", *Building and Environment*, Vol. 30, No. 1, pp. 129-133.

Murakami, S., Kato, S., 1989, "Numerical and Experimental Study on Room Airflow — 3-D Predictions using the *k–ε* Turbulence Model, Building and Environment, Vol. 24, No. 1, pp. 85-97.

Nielsen, P.V., 1994, "Stratified flow in a room with displacement ventilation and wall-mounted air terminal devices", *ASHRAE Transactions: Symposia*, NO-94-16-2, pp. 1163-1169.

Ohira, N., Kato, S. and Murakami, S., 2000, "CFD analysis of thermal plume and indoor airflow using *k–ε* models with buoyancy effect" 3rd symposium on turbulence heat and mass transfer, Nagoya, Japan, 2-6 April 2000.

Peng, S.H., Holmberg, S and Davidson, L., 1997, "On the Assessment of Ventilation Performance with the Aid of Numerical Simulations", *Building and Environment*", Vol. 32, No. 6, pp. 497-508.

Redondo, J.M., Sanchez, M.A. and Cantalapiedra, I.R., 1996, "Turbulent mechanisms in stratified fluids", Dynamics of Atmospheres and Oceans, Vol. 24, pp. 107-115.

Skistad, H., 1998, “Utilizing selective withdrawal in the ventilation of large rooms: select-vent” in: Room Vent Conference, Stockholm, June.

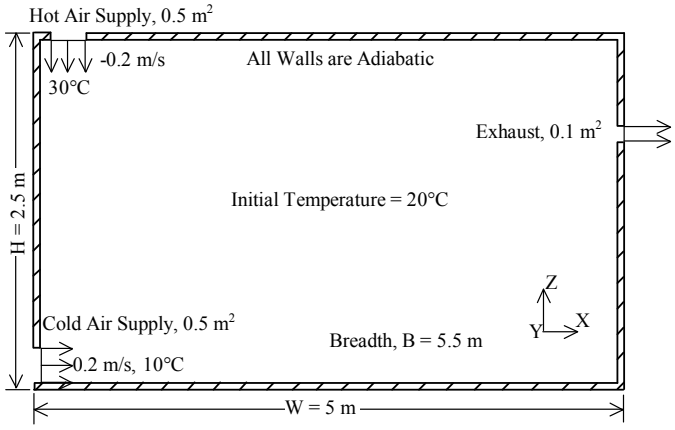

Schematic 1. CROSS-SECTION OF THE MODEL.

Table 1. REYNOLDS NUMBER RELATION.

T [°C]	$\mu \times 10^{-5}$ [kg/ms]	$Re \times 10^3$ (U_S=0.2 m/s)	$Re \times 10^4$ (U_S=0.4 m/s)	$Re \times 10^4$ (U_S=0.8 m/s)	$Re \times 10^4$ (U_S=1.6 m/s)
10	1.7643	7.0710	1.4142	2.8284	5.6568
20	1.8126	6.6475	1.3295	2.6590	5.3180
30	1.8602	6.2637	1.2527	2.5055	5.0110
40	1.9071	5.9146	1.1829	2.3658	4.7317

Table 2. ARCHIMEDES NUMBER RALATION.

No.	U_0 [m/s]	T_C [°C]	T_H [°C]	ACH	Ri	Ar
1	0.2	10	30	0.9555	40.4703	57.6130
2	0.4	10	30	1.8459	10.1176	14.4032
3	0.8	10	30	3.5699	2.5294	3.6008
4	1.6	10	30	6.9117	0.6323	0.9002

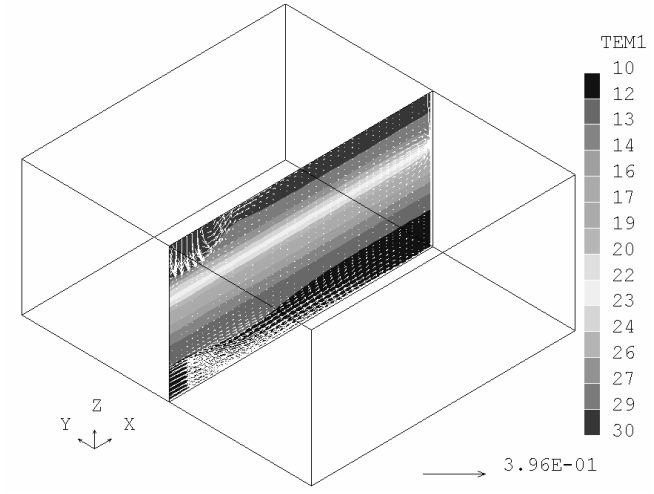

(a) INLET VELLOCITIES = 0.2 m/s

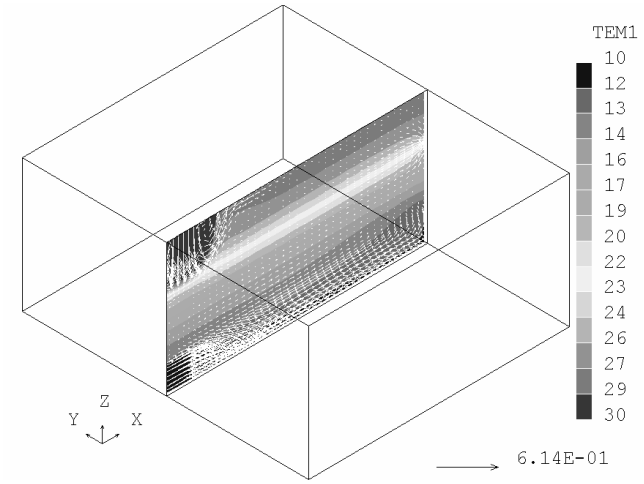

(b) INLET VELLOCITIES = 0.4 m/s

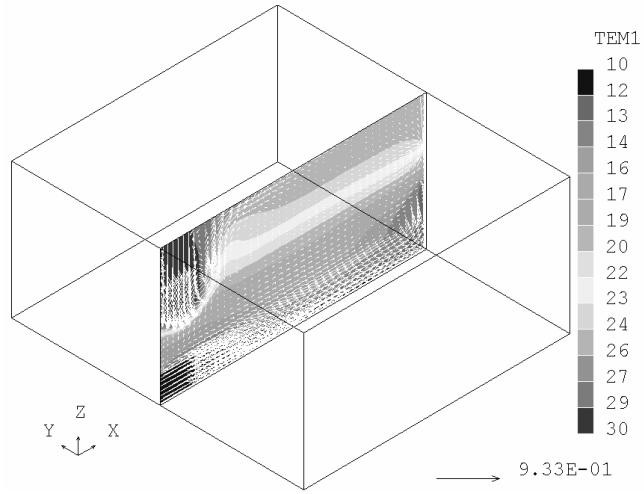

(c) INLET VELLOCITIES = 0.8 m/s

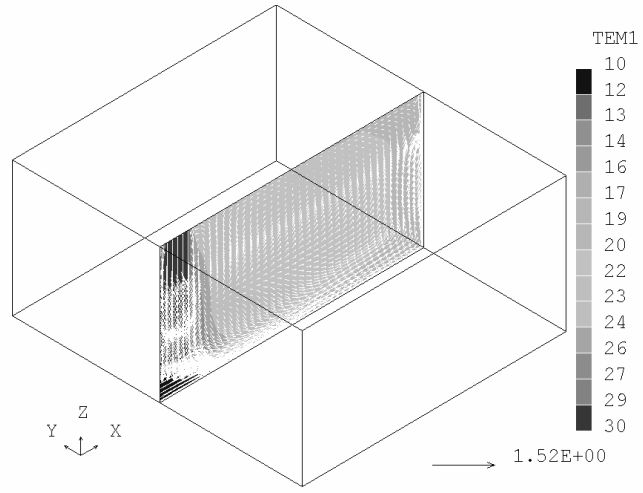

(d) INLET VELLOCITIES = 0.2 m/s

Figure 1. THE EFFECT OF INCREASING THE INLET VELOCITY WHILE KEEPING A CONSTANT HEIGHT. IN ALL CASES THE *K–ε* MODEL IS USED. THE RESULTS FROM THE OTHER MODELS ARE SIMILAR.

(a) EXTRACT HEIGHT = 0.8 m

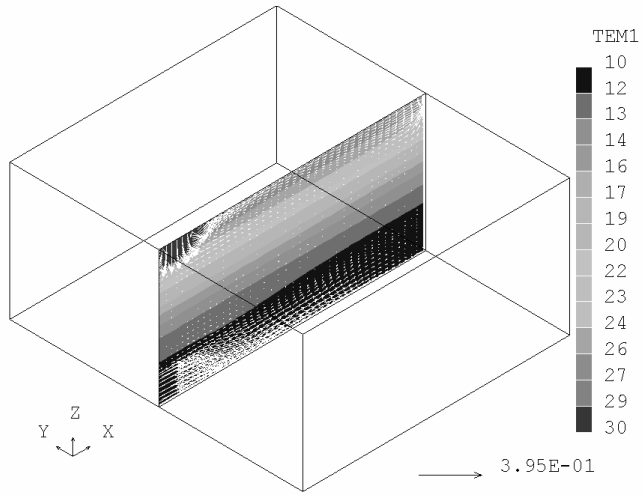

(b) EXTRACT HEIGHT = 0.8 m

Figure 2. THE EFFECT OF EXTRACT HEIGHT WHILE KEEPING CONSTANT THE INLET VELOCITY WHILE KEEPING A CONSTANT HEIGHT. IN ALL CASES OF THIS FIGURE THE *K–ε* MODEL IS USED. THE RESULTS FROM THE OTHER MODELS ARE SIMILAR.

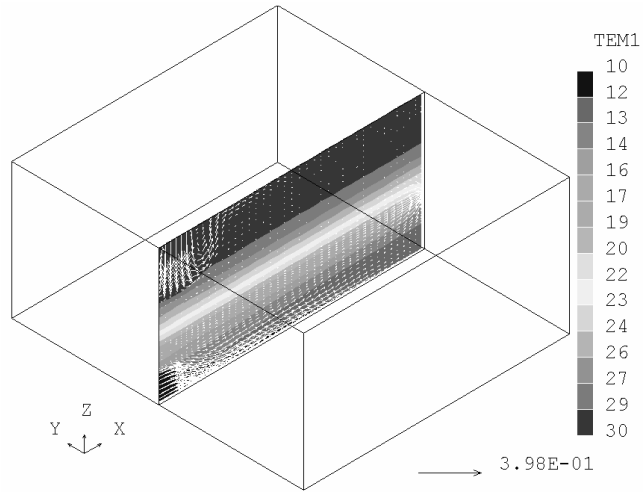

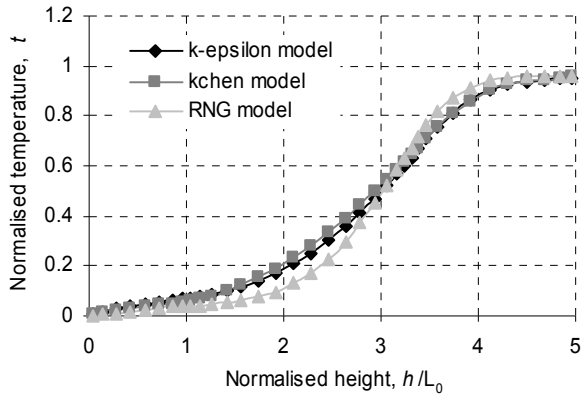

(a) INLET VELLOCITIES = 0.2 m/s

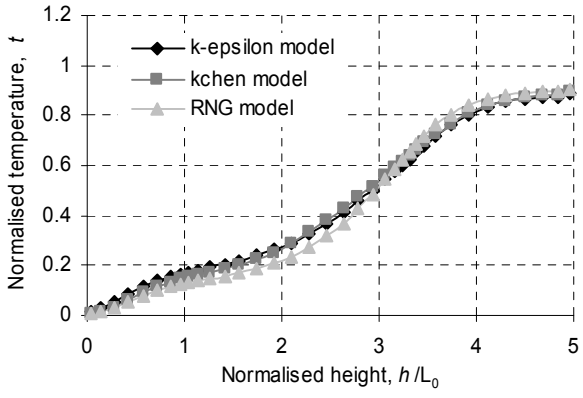

(b) INLET VELLOCITIES = 0.4 m/s

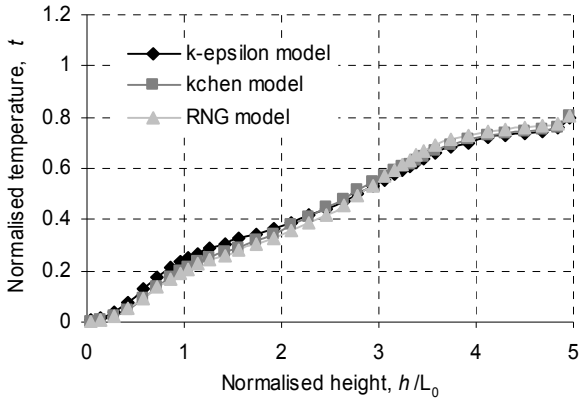

(c) INLET VELLOCITIES = 0.8 m/s

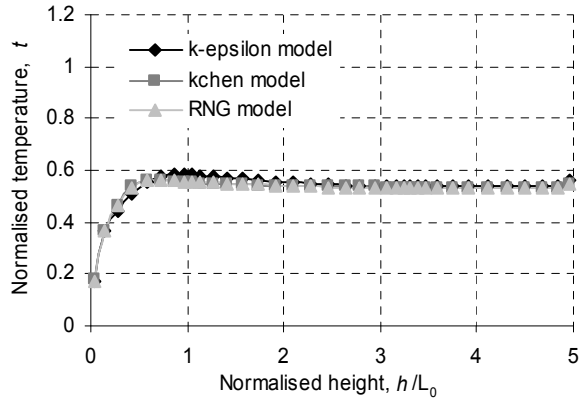

(d) INLET VELLOCITIES = 1.6 m/s

Figure 3. NON-DIMENSIONAL VERTICAL TEMPERATURE VARIATION IN THE MIDDLE OF THE ROOM VERSUS NON-DIMENSIONAL HEIGHT VARYING INLET VELOCITIY. INLET TURBULENCE INTENSITY = 20%.

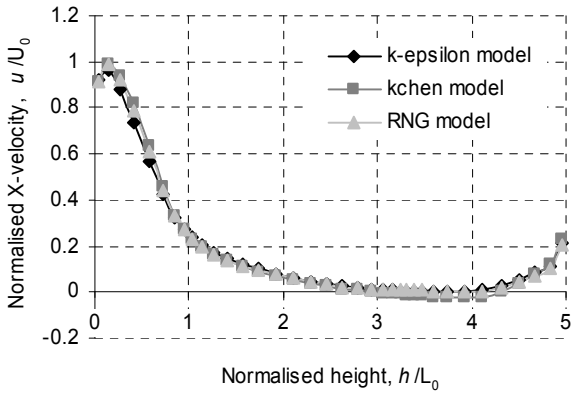

(b) INLET VELLOCITIES = 0.8 m/s

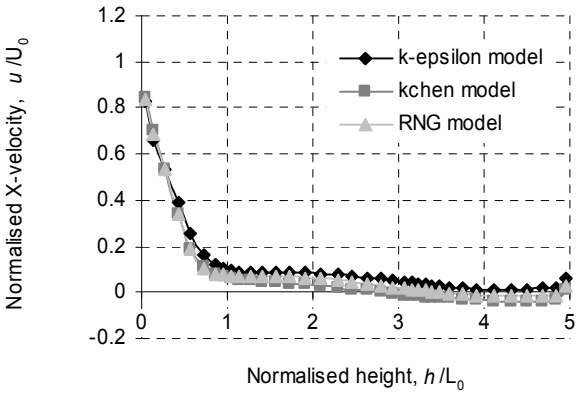

(c) INLET VELLOCITIES = 1.6 m/s

Figure 4. NON-DIMENSIONAL X-VELOCITY VARIATION IN THE MIDDLE OF THE ROOM VERSUS NON-DIMENSIONAL HEIGHT VARYNG INLET VELOCITY. TURBULENCE INTENSITY = 20%.

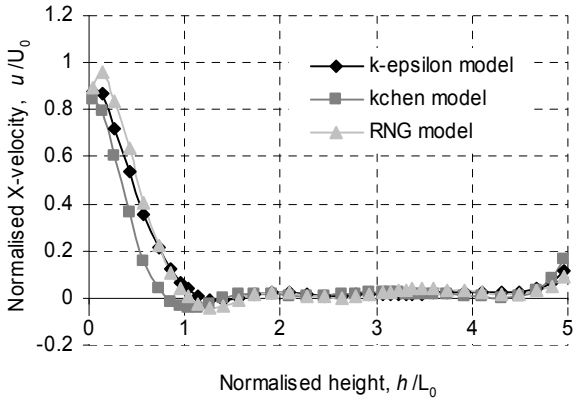

(a) INLET VELLOCITIES = 0.2 m/s

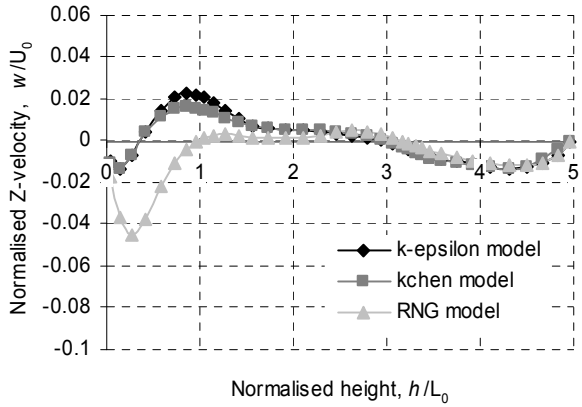

(a) INLET VELLOCITIES = 0.2 m/s

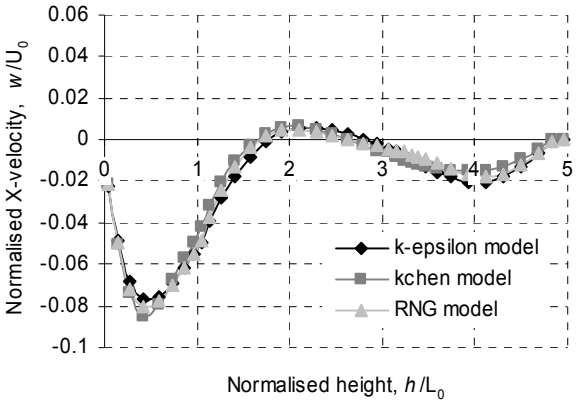

(b) INLET VELLOCITIES = 0.8 m/s

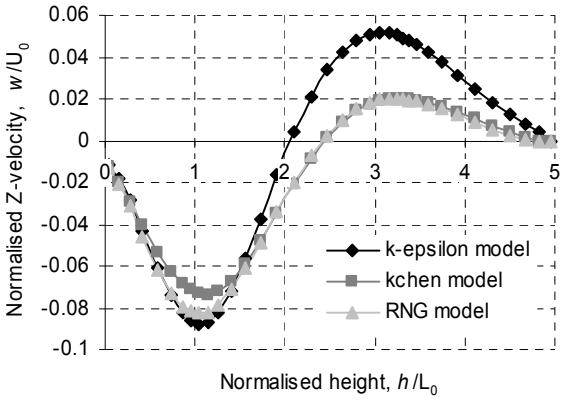

(c) INLET VELLOCITIES = 1.6 m/s

Figure 5. NON-DIMENSIONAL VERTICAL VELOCITY VARIATION IN THE MIDDLE OF THE ROOM VERSUS NON-DIMENSIONAL HEIGHT VARYING INLET VELOCITY. INLET TURBULENCE INTENSITY = 20%.

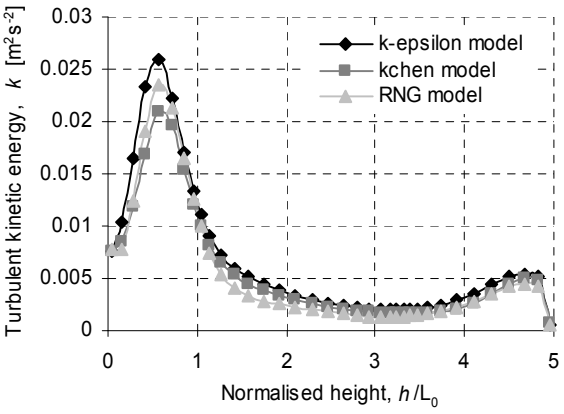

(b) INLET VELLOCITIES = 0.8 m/s

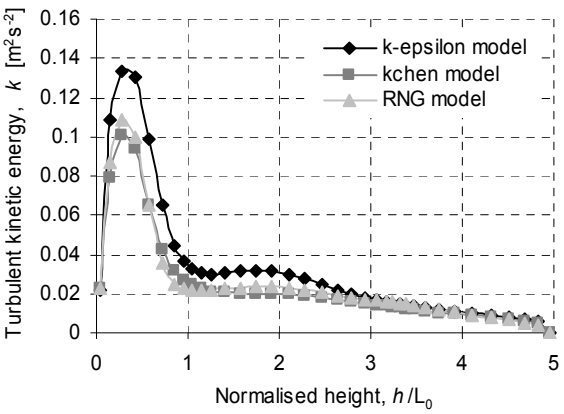

(c) INLET VELLOCITIES = 1.6 m/s

Figure 6. KINETIC ENERGY VARIATION IN THE MIDDLE OF THE ROOM VERSUS NON-DIMENSIONAL HEIGHT VARYING INLET VELLOCITY. INLET TURBULENCE INTENSITY = 20%.

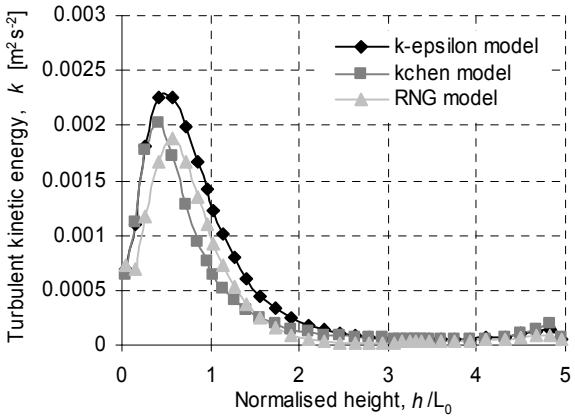

(a) INLET VELLOCITIES = 0.2 m/s